

Green Power Based Power Supply System

Blessy A Rahiman¹

¹*Electrical and Electronics Engineering Department, Musaliar College of Engineering and Technology,
Pathanamthitta, Kerala, India*

Abstract- In the near future, some fuel cell systems could be an accessible and attractive alternative to conventional electricity generation. Renewable energy systems have developed wide interest to supply electricity in remote areas as well as for distributed power generation particularly during peak loads. Fuel-cell-based power generation is also gaining popularity in residential applications as well as distributed power generation due to its cleanliness, portability, and suitability for electricity and heat generation. Development of a suitable power electronic interface to make the technology viable is still a challenge. This paper presents modeling, simulation, and experimental study of a fuel cell (FC) power plant (FCPP) suitable for stand-alone application as well as for microgrid / grid interface using different controllers like PI Controller, PID Controller and Fuzzy Logic Controllers. A single-stage pulsewidth modulation inverter is selected as power electronic interface between FC and grid. A mathematical model is developed in per unit system to define the power limits in terms of FC, converter, and power system parameters. The simulation model is developed in MATLAB environment with control scheme implementation in dq reference frame for investigation. A comparative assessment of the three different controllers is brought out.

Keywords- Distributed generation, fuel cell (FC), grid interface, power conditioning unit, power quality, pulsewidth modulation (PWM) inverter, stand-alone system.

I. INTRODUCTION

Rapid growth in energy consumption during the last century on the one hand, and limited resources of energy on the other, has caused many concerns and issues today. Although the conventional sources of energy, such as fossil fuels, are currently available in vast quantities, however they are not unlimited and sooner or later will vanish. Moreover, environmental concerns, such as global warming, are becoming increasingly serious, and require significant attention and planning. Renewable energy sources are the answer to these needs and concerns, since they are available as long as the sun is burning, and because they are sustainable as they have no or little impact on the environment. One technology which can be based upon sustainable sources of energy is fuel cell.

Fuel cells are devices that directly convert the chemical energy stored in some fuels into electrical energy and heat. The preferred fuel for many fuel cells is hydrogen, and hydrogen fuel is a renewable source of energy; hence fuel cell technology has received a considerable attention in recent years.

Since the FC delivers dc power, it must be inverted and stepped up to be able to use for household applications as well

as for distributed generation. Another serious problem with FC is that its voltage decreases almost linearly with the increase in load current; hence, output voltage must be regulated at a desired level. Therefore, a suitable power electronic interface is required between FC and load/grid, with the capabilities of FC voltage regulation, output voltage matching, and galvanic isolation between FC and load/grid.

The aforementioned tasks can be achieved either by connecting a dc–dc converter with voltage gain to the FC followed by a dc/ac inverter or by directly connecting an inverter to the FC followed by a step-up transformer as shown in Fig. 1. Several topologies of switched-mode dc–dc converter followed by inverter are proposed and compared based on their performance [8]–[14]. A switched-mode dc–dc converter is preferred to limit the size and cost of the system followed by a grid-connected inverter [8]. A current-fed dc–dc converter is preferred over a voltage-fed dc–dc converter as the former requires reduced input filtering. A push–pull dc–dc converter is selected with voltage gain [8], [10], [11] to reduce the switch conduction losses. However, its use is restricted to low- and medium-power applications. Full-bridge topology is preferred for high-power applications as push–pull topologies have a serious problem of center tap termination, which tends to cause saturation of the transformer at high-power levels [9]. However, a full-bridge topology requires more switches but of half rating, which is more economical and efficient [9], [12], [13].

All these topologies discussed earlier use multiple-stage conversion to deal with the aforementioned challenges, which results in large component count and, therefore, poor reliability, additional cost, and low efficiency. In addition to this, energy storage devices such as battery and ultra capacitors are also needed at various stages [9], [10] either to supply auxiliaries or to improve the slow transient response of the FC.

Direct connection of dc/ac inverter to the FC with ac gain has only one conversion stage [15]. This topology offers the advantages of least component count and low losses. Also, single conversion facilitates reverse power flow from grid particularly during start-up to supply the auxiliaries. The step-up transformer provides the isolation between FC

and load as well. Grid interface of renewable power sources like FC is one of the probable area of research particularly during peak loads [16]. However, complete design, mathematical modeling, and implementation of control scheme are some of the issues that need more focused attention.

This paper presents modeling and simulation of a single stage power electronic interface between FC and load/grid. A mathematical model of the FC-based power supply system is developed in qd0 reference frame in terms of FC, converter, and power system parameters. This model is used to define the active and reactive power limits, which can be supplied by the system to facilitate grid interface. The model is developed in per unit (p.u.) system which can be further extended for grid connected environment. The topology selected can also be used for bidirectional conversion to supply the auxiliaries from the grid initially for start-up. A Nexa™ proton exchange membrane (PEM) FC of 1.2 kW is considered for the design and study. The I–V characteristics of the FC are obtained considering the effect of temperature and hydrogen pressure. After comparing the simulated characteristics with experimentally obtained I–V characteristics, a simplified model of FC is developed based on its practical characteristic in linear region. The simulation model is developed in MATLAB–Simulink and Sim Power- Systems environment. Control scheme is implemented in qd0 stationary reference frame, and various simulation results are presented in steady state as well as during transients.

II. FUEL CELL

Proton Exchange Membrane fuel cells (PEMFC) are electrochemical energy conversion devices that convert the chemical energy of supplied reactants (hydrogen and oxygen) into electricity. To summarize the operation simply, reactant gases are supplied to both electrodes of the fuel cell via the channels, the gas diffusion layer facilitates even distribution to the catalyst-coated membrane, and the catalyst accelerates the oxidation and reduction of the reactants, which are the primary reactions desired for fuel cell operation as shown in Figure 1

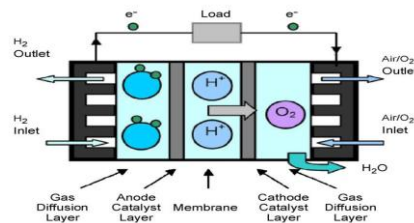


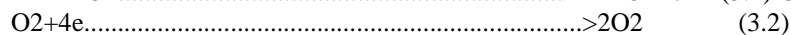
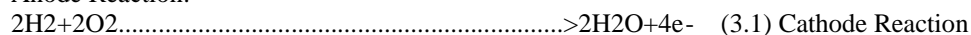
Figure:.1 Schematic representation of fuel cell chemistry.

The oxidation on the anode side of the membrane releases two electrons, which then traverse the circuit to satisfy the load required of the cell, while the remaining protons (H+) travel through the membrane to the cathode side. The O₂ reduction on the cathode side splits the oxygen molecule, which then joins with the electrons completing the circuit and the protons from the membrane to form product water H₂O

2.1 Reactions in Fuel cell

The reactions in a fuel cell are

Anode Reaction:



Overall Reaction



2.2 Advantages of fuel cells

1. They transform the fuel chemical energy into electric power with 60% efficiency which is considered to be twice that of traditional generating stations.
2. The absence of moving parts in fuel cell's operation, except for air blowers (for O₂) and (for H₂) and /or water pumps, result in very low noise levels, relatively higher efficiency and emits lower air pollutants.
3. No combustion is involved in the fuel cell operation that makes it an environmentally friendly generation with approximately negligible emission of CO₂.

2.3 Disadvantages of fuel cells

The main disadvantage of fuel cell is that aging of fuel cell causes the internal impedance to increase slowly and therefore in order to regulate the output voltage a power electronic interface is required, which increases the cost.

III. FUEL CELL POWER SUPPLY SYSTEM

The single-line diagram of the proposed single-stage FC based power supply system is shown in Fig. 3.2. A single-stage PWM inverter followed by a low-pass filter is used with a Nexa™ PEM FC. Since FC operates in low voltage range (26–48 V) and load/grid voltage is relatively high (415Vrms), a step-up transformer is used to meet the desired voltage level. It also provides the isolation between FC and load.

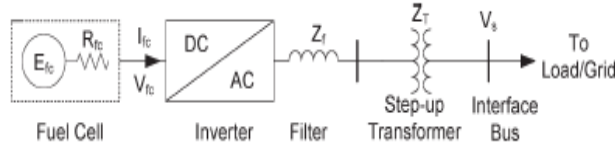


Figure: 2 Single line diagram of Fuel cell power plant

IV. SYSTEM DESIGN

4.1 FC Model

The performance of the FC is improved by thermodynamics and electrical efficiency of the system. The thermodynamic efficiency depends upon the fuel processing, water management, and temperature control of the system. However, the electrical efficiency depends on the various losses over the FCs like ohmic loss, activation loss, and concentration loss. In reality, the FCs differ in terms of characteristics, material used in construction, and their suitability of applications. Hence, the development of an accurate FC model is very important. PEM FC models are reported in the literature based on the thermodynamic and electrochemical equations. A mathematical approach is presented for building a dynamic model for a PEM fuel-cell stack.

The proportional relationship of the flow of gas through a valve with its partial pressure can be expressed as

$$\frac{q_{H_2}}{P_{H_2}} = KH_2 \quad (3.4)$$

$$\frac{q_{H_2O}}{P_{H_2O}} = KH_{2O} \quad (3.5)$$

For hydrogen, there are three relevant contributions to the hydrogen molar flow: the input flow, the flow that takes part in the reaction and the output flow. The relationship among these factors can be written as:

$$\frac{d}{dt} P_{H_2} = \left(\frac{RT}{V_{an}} \right) * (q_{H_2 \text{ in}} - q_{H_2 \text{ out}} - q_{H_2 \text{ r}}) \quad (3.6)$$

According to the basic electrochemical relationship between the hydrogen flow and the stack current can be written as :

$$q_{H_2} = \frac{NI}{2F} = 2K_r IFC \quad (3.7)$$

The polarization curve for the PEM fuel cell is obtained from the sum of the Nernst's voltage, the activation over voltage η_{act} , and the ohmic over voltage η_{ohmic} . Assuming constant temperature and oxygen concentration, the fuel cell output voltage may be expressed as

$$V_{cell} = E + \eta_{act} + \eta_{ohmic} \quad (3.8)$$

The FC stack voltage under loaded condition (V_{dc_stack}) is a function of activation loss (V_{act}), concentration loss (V_{con}), and ohmic loss (V_{ohmic}) and is given by Nernst equation:

$$V_{dc_stack} = V_{open} - V_{ohmic} - V_{act} - V_{con} \quad (3.9)$$

Based on this, a dynamic model of Ballard 1.2-kW FC is developed in MATLAB/Simulink. It can be seen that, at low current level, the ohmic loss becomes less significant and the increase in output voltage is mainly due to activity of slowness of chemical reactions. At very high current density, the voltage fall down significantly because of the reduction of gas exchange efficiency. This is mainly due to over flooding of water in catalyst. Intermediate between the active region and concentration region, there is a linear slope which is Figure.3

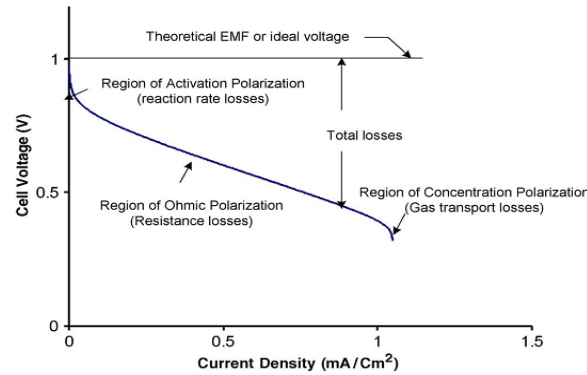


Figure: 3. Polarisation characteristics of fuel cell

4.2 Simplified Model

The simplified model represents a particular fuel cell stack operating at nominal conditions of temperature and pressure. A diode is used to prevent the flow of negative current into the stack. This model is based on the equivalent circuit of a fuel cell stack shown in Figure.4.

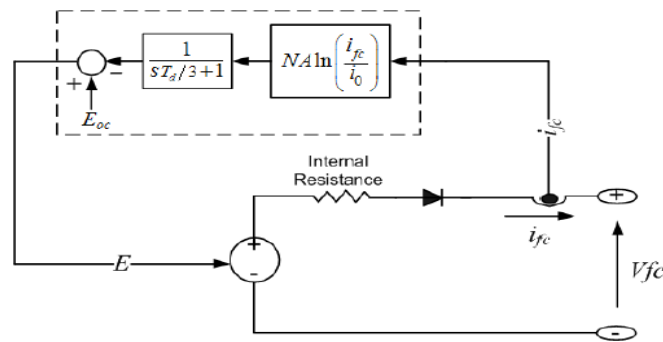


Figure: 4. Equivalent circuit of fuel cell stack

4.3 Filter Design

An LC filter is connected before the step-up transformer to filter out the harmonics present in the inverter output. For a switching frequency around 4860 Hz, the lowest order harmonic available in the inverter output is in the range of 4740 Hz. Therefore, the cutoff frequency of LC filter can be selected as 1200 Hz, which is 20 times greater than the fundamental frequency and almost four times lower than the switching frequency (4860 Hz), so as not to attenuate the fundamental frequency. The resonance frequency can be expressed as

$$f_c = 1/2\pi\sqrt{L_f C_f} = 1200 \text{ Hz.} \quad (3.11)$$

Based on the aforementioned expression, different combinations of filter components are taken. Considering a cutoff frequency of 1200 Hz, Q factor of 30, THDV and THDI that are less than 5%, and inductor power loss < 1%.

4.4 Selection of P.U. Values

4.4.1 AC-Side Base Values

The FC nominal power expressed in volt amperes is selected as the base power for the purpose of defining the base p.u. values. RMS values of the rated phase voltage are generally selected as the base voltage for abc variables, whereas peak values are selected for qd variables. However, as the p.u. values remain the same in both systems, the rms value of line-to-neutral voltage is preferred here to normalize the voltage, as system variables are generally defined in rms values. The fundamental rated frequency is considered as the base frequency. All other base values are derived from the aforementioned independent base values given hereinafter

$$\text{base VA } S_b = P_{\text{nomfc}} [\text{VA}] \quad (3.12)$$

$$\text{base voltage } V_{b,ac} = V_{\text{nomrms}}(\text{LN}) [\text{V}] \quad (3.13)$$

$$\text{base current } I_{b,ac} = S_b / 3V_{b,ac} [\text{A}] \quad (3.14)$$

$$\text{base impedance } Z_b = V_{b,ac} / I_{b,ac} = 3\sqrt{2} V_{b,ac} / S_b [\Omega]. \quad (3.15)$$

4.4.2 FC Base Values

The proposed FC base quantities (dc) are derived from the voltage source converter with SPWM modulation. The ac-side line-to-neutral rms voltage is proportional to the dc-side FC voltage as

$$V_{rmsac,LN} = 1/2\sqrt{2}m_a V_{dc} \quad (3.16)$$

where m_a is the amplitude modulation .

Assuming a lossless converter, FC base voltage and current can be obtained by equating the powers at ac and dc sides of the inverter, operating at unity power factor ($\cos\phi = 1$) and $m_a = 1$, as

$$P_{ac} = 3V_{ac}I_{ac}\cos\phi = V_{dc}I_{dc} = P_{dc} \quad (3.17)$$

$$V_{b,fc} = V_{dc} = 2\sqrt{2}V_{ac} \text{ [V]} \quad I_{b,fc} = 3/2\sqrt{2}I_{ac} \text{ [A]}. \quad (3.18)$$

E Steady-State Model of FCPP

Inverter-Side (AC Side) Equations

The steady-state model of FCPP is developed in qd reference frame to define the power limits in terms of converter and FC parameters. The symmetrical, balanced, and three-phase voltages at converter, transformer, and utility bus C, T, and S, can be expressed as

$$v_{i,abc} = [v_{i,a} \ v_{i,b} \ v_{i,c}]^T \quad T_i \in [C,T,S] \\ = V_i [\cos(\omega t + \theta_{i0}) \cos(\omega t + \theta_{i0} - 2\pi/3) \cos(\omega t + \theta_{i0} + 2\pi/3)] \quad T_i \in [C,T,S] \quad (3.19)$$

where V_C , V_T , and V_S are the amplitudes, $\omega_C = \omega_T = \omega_S = \omega_e$ are the synchronous frequencies, θ_{C0} , θ_{T0} , and θ_{S0} are the initial angular displacements at buses C, T, and S, respectively, and the matrix superscript T denotes the matrix transpose. Equation (3.19) can be transformed into an arbitrary dqo reference frame rotating synchronously ($\omega = \omega_e$) having initial angular displacement θ_0

$$v_{i,qd0} = [v_{i,q} \ v_{i,d} \ v_{i,0}]^T \quad T_i \in [C,T,S] \\ = V_i [\cos(\theta_{i0} - \theta_0) \ -\sin(\theta_{i0} - \theta_0) \ 0]^T. \quad (3.20)$$

The zero component does not exist in a symmetrical system; thus, (3.20) can be written in converter's qd reference frame

($\omega = \omega_C$) as

$$v_{Cqd} = [V_C \ 0]^T \quad (3.21)$$

$$v_{CSqd} = [V_S \cos\delta_{CS} \ V_S \sin\delta_{CS}]^T \quad (3.22)$$

where $\delta_{CS} = \theta_{C0} - \theta_{S0}$.

Voltage at bus C can be expressed as a function of the voltage at the bus S, current, and system impedance expressed in the converter's qd reference frame

$$v_{Cqd} = Z_{dq} i_{dq} + v_{CSqd} \quad (3.23)$$

The current can be expressed in the converter's qd reference frame as

$$\begin{bmatrix} i_q \\ i_d \end{bmatrix} = \frac{1}{Z} \begin{bmatrix} V_C \sin\gamma + V_C \sin(\delta_{CS} - \gamma) \\ V_C \cos\gamma - V_C \cos(\delta_{CS} - \gamma) \end{bmatrix} \quad (3.24)$$

where $R = R_T + R_S$, $X = X_T + X_S$, $Z = \sqrt{R^2 + X^2}$ and $\gamma = \pi/2 - \tan^{-1} X/R$.

Power at the converter bus C can be expressed as

$$\begin{bmatrix} P_C \\ Q_C \end{bmatrix} = \begin{bmatrix} V_C & 0 \\ 0 & V_C \end{bmatrix} \begin{bmatrix} i_q \\ i_d \end{bmatrix} \quad (3.25)$$

On putting i_q and i_d from (3.24), active and reactive powers at converter bus can be expressed

$$\begin{bmatrix} P_C \\ Q_C \end{bmatrix} = \frac{1}{Z} \begin{bmatrix} V_C^2 \sin\gamma + V_C V_S \sin(\delta_{CS} - \gamma) \\ V_C^2 \cos\gamma - V_C V_S \cos(\delta_{CS} - \gamma) \end{bmatrix} \quad (3.26)$$

If the ratio X/R is large (>10), $\gamma \rightarrow 0$; thus, (3.26) can be simplified to

$$\begin{bmatrix} P_C \\ Q_C \end{bmatrix} = \frac{1}{X} \begin{bmatrix} V_C V_S \sin\delta_{CS} \\ V_C^2 - V_C V_S \cos\delta_{CS} \end{bmatrix} \quad (3.27)$$

Equation (3.27) is known as power expressions for sending and receiving end nodes interconnected with the impedance Z or reactance X, respectively.

4.4.3 FC-Side (DC Side) Equations:

As validated above from the approximate linearized equivalent circuit, the FC voltage can be expressed in terms of FC current and resistance as

$$V_{fc} = E_{fc} - R_{fc} i_{fc} \quad (3.28)$$

where E_{fc} and R_{fc} are constant for an operating condition. Equation (3.28) is valid for $i_{fc} \in [0, i_{fc,max}]$, for $i_{fc} \geq i_{fc,max}$,
 $V_{fc} \rightarrow 0$.

As the converter's switching frequency is very high as compared to fundamental frequency, the fast average value of the converter voltage $\hat{v}_{C,abc}$ can be defined as the average value over the switching period, in terms of the modulation index

“ m_a ” and dc-side voltage V_{fc}

$$\hat{v}_{C,abc} = v_{C,abc} = m_a V_{fc} [\cos(\theta_C) \cos(\theta_C - 2\pi/3) \cos(\theta_C + 2\pi/3)]^T \quad (3.29)$$

The fast average converter voltage can be expressed in the converter's qd reference frame ($\omega = \omega_C$) by dropping the superscript for simplicity

$$V_{Cqd} = \begin{bmatrix} V_{Cq} \\ V_{Cd} \end{bmatrix} = \begin{bmatrix} V_C \\ 0 \end{bmatrix} = \begin{bmatrix} m_a V_{fc} \\ 0 \end{bmatrix} \quad (3.30)$$

Assuming a lossless converter, active power is equal on both sides of the converter

$$P_C = P_{fc}$$

$$\text{i.e. } m_a V_{fc} i_{fc} = V_{fc} i_{fc} \quad (3.31)$$

$$\text{or } i_{fc} = m_a i_q \quad (3.32)$$

Power Equations in Terms of System Parameters:

The active and reactive powers at converter bus “C” can be expressed as

$$\begin{bmatrix} P_C \\ Q_C \end{bmatrix} = \begin{bmatrix} V_{Cq} i_q + V_{Cd} i_d \\ V_{Cq} i_d - V_{Cd} i_q \end{bmatrix} = \begin{bmatrix} V_{Cq} i_q \\ -V_{Cd} i_d \end{bmatrix} = \begin{bmatrix} V_C i_q \\ -V_C i_d \end{bmatrix} \quad (3.33)$$

$$\begin{bmatrix} P_C \\ Q_C \end{bmatrix} = \begin{bmatrix} m_a E_{fc} i_q - m_a^2 E_{fc} i_q^2 \\ m_a E_{fc} i_d - m_a^2 R_{fc} i_q i_d \end{bmatrix} \quad (3.34)$$

Active and reactive powers converter bus “C” (P_C, Q_C, V_C) can be expressed as a function of the system variables—FC (R_{fc}, E_{fc}), converter (R_{fc}, E_{fc}), filter and transformer (Z_f, Z_T), and utility (V_S, Z_S).

V. CONVERTER TOPOLOGY AND CONTROL SCHEME

5.1 Basic Scheme and Power Converter Topology

The single-line diagram of the proposed single-stage fuel cell based power supply system is shown in Fig.2. A single-stage PWM inverter followed by a low-pass filter is used with a 1.2-kW 48-V Nexa™ PEM FC. Since FC operates in low voltage range (26–48 V) and load/grid voltage is relatively high a step-up transformer is used to meet the desired voltage level. It also provides the isolation between FC and load.

A single-bus six-switch voltage source PWM bridge converter used for dc–ac conversion is preferred here for three-phase application suitable for grid interface. A low-pass LC filter is used at the PWM inverter output to achieve better harmonic reduction in the phase current and inverter output voltage. Inverter-side placement of filter results in high current rating of the filter inductor, whereas capacitors are rated at a reduced voltage. As the load increases, FC voltage decreases. In order to operate the FC efficiently, the flow rate of hydrogen must be adjusted with the change in load. However, depending on the type of FC system, this flow change is a very slow process and has time constant as large as 30 s. Therefore, some type of energy storage is required.

5.2 Control Strategy

As the FC voltage is usually very small, around 1.2 V, it becomes necessary to stack many cells that need to be connected in cascaded series and parallel form to increase its power capacity. A typical FC polarization characteristic is shown in Fig. 3. It is observed that a linear region exists where FC voltage drops as the current density increases due to its ohmic nature. This region is observed mainly due to internal resistance offered by various components, called ohmic polarization. At low current level, the ohmic loss becomes less significant; the

increase in output voltage is mainly due to activity of the chemical reactions (time taken for warm-up period). Thus, this region is also called active polarization. At very high current density, the voltage fall down significantly because of the reduction of gas exchange efficiency; it is mainly due to over flooding of waters in catalyst, and this region is also called concentration polarization . This reduction in the FC voltage with increase in current drawn (output power), keeping constant the hydrogen flow rate, can be regulated by controlling the modulation index (m_a) of the PWM inverter as shown by

$$V_{ac} = m_a \cdot V_{dc} \angle \delta \quad (4.1)$$

where V_{ac} is the ac output voltage, V_{dc} is the FC output voltage, m_a is the inverter modulation index, and δ is the inverter phase angle .

As control of magnitude of the output voltage is not enough to meet the active power requirement of the load, the phase angle of the inverter “ δ ” should also be controlled. These two variables (m_a and δ) are used to control the transient power adjustments. Hydrogen flow rate must be adjusted to control the steady-state power requirement. Output voltage is compared to the reference voltage command to control the modulation index “ m_a ” , which ultimately regulates the inverter output voltage and reactive power flow as well. In order to control the reactive power flow in grid-connected environment, voltage is compared with the reference voltage and processed in proportional–integral (PI) controller, PID and Fuzzy Logic Controller to control the inverter output voltage.

VI. SIMULATION RESULTS

The simulation model for the control of converter parameters (m_a and δ) in closed loop is developed in MATLAB environment. The FC voltage is applied to the MOSFET inverter through a dc link capacitor. The MOSFET inverter is controlled using SPWM at 4.86-kHz carrier frequency. The circuit is discretized at a sample time of $1 \mu s$. The output of PWM inverter is applied to a step-up transformer after filtering. The load voltage is regulated at 1 p.u. (415 Vrms) by PI, PID and fuzzy voltage regulator using abc-to-dq and dq-to-abc transformations. The output of the voltage regulator is multiplied by the reference sine vector to generate the three modulating signals used by the PWM generator to generate the firing pulses.

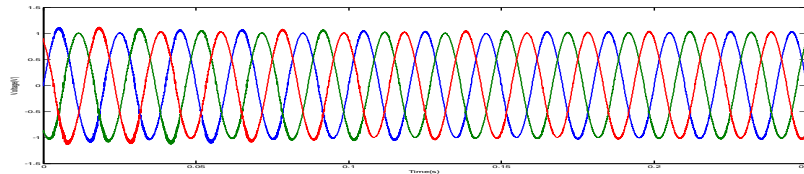


Figure:5 Three phase output voltage after filtering with PI controller.

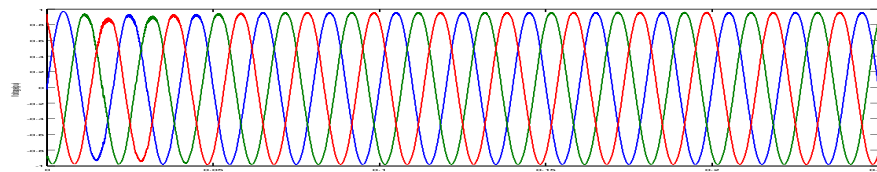


Figure:8 Three phase output voltage after filtering with PID controller.

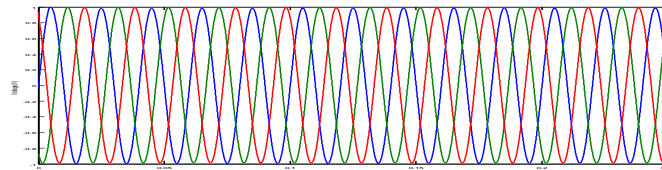


Figure:11. Three phase output voltage after filtering with Fuzzy Logic Controller.

VII. COMPARISON BETWEEN THREE CONTROL STRATEGIES

Results of two control schemes are summarized in the table below. From the table we can conclude that % THD reduces more with Fuzzy logic controller. With PI controller THD is reduced from 83.72% to 1.77% after filtering. With PID controller THD is reduced from 99.88% to 1.14% after filtering . With fuzzy controller THD is reduced from 89.88% to 0.47% after filtering .Settling time is also minimum with Fuzzy logic controller.

SL NO	ControllerUsed	THD(%)	Settling Time(s)
1	PI Controller	1.77	0.15
2	PID Controller	1.14	0.07
3	Fuzzy Controller	0.47	0.01

VIII. CONCLUSION

The proposed single-stage power electronic interface regulates the variation in FC voltage for a corresponding change in load by changing the modulation index and phase angle. The THD values of output voltage is maintained 0.47% using fuzzy logic controller, making the system suitable for grid interface/standalone use. Based on the simulation it can be concluded that the modulation index adjusts to account the FC drooping characteristics for any variation in load with significantly good transient response. Also, the inverter output voltage is synchronized with grid voltage making the system suitable for grid interface. It can be concluded that fuzzy logic controller is the best controller for the system as THD can be reduced from a high value to a low value after filtering and settling time is minimum.

IX. REFERENCES

- [1] Shailendra Jain, Jin Jiang, Xinhong Huang, Member and Srdjan Stevandic, "Modeling of Fuel-Cell-Based Power Supply System for Grid Interface" Proc. IEEE, vol.48, no.4, pp. 1142- 1153, july/august 2012
- [2] M. Farooque and H. C. Maru, "Fuel cell the clean and efficient power generators," Proc. IEEE, vol. 89, no. 12, pp. 1819–1829, Dec. 2001..
- [3] M. L. Perry and S. Kotso, "A back-up power solution with no batteries," in Proc. IEEE IEEE Telecommun. Energy Conf., Sep. 19–23, 2004, pp. 210–217.
- [4] M. W. Ellis, M. R. Von Spakovsky, and D. J. Nelson, "Fuel cell systems:Efficient,flexible energy conversion for the 21st century," Proc. IEEE, vol. 89, no. 12, pp. 1808–1818, Dec. 2001.
- [5] M. C. Williams, "Fuel cells and the world energy future," in Proc. IEEE-PES Summer Meeting, Vancouver, BC, Canada, Jul. 15–19, 2001, pp. 725–730.
- [6] J. Anzicek and M. Thompson, "DC–DC boost converter design for Kettering University’s gem fuel cell vehicle," in Proc. IEEE Elect. Insul. Conf., 2005, pp. 307–316.
- [7] W. Gao, "Performance comparison of a fuel cell-battery hybrid powertrain and a fuel cell-ultracapacitor hybrid powertrain," IEEE Trans. Veh. Technol., vol. 54, no. 3, pp. 846–855, May 2005.
- [8] K. Rajashekara, "Power conversion and control strategies for fuel cell vehicles," in Proc. IEEE IECON, Nov. 2–6, 2003, vol. 3, pp. 2865–2870.
- [9] G. K. Andersen, C. Klumpner, S. B. Kjtter, and F. Blaabjerg, "A newgreen power inverter for fuel cells," in Proc. PESC, Jun. 23–27, 2002, pp. 727–733.
- [10] T. A. Nergaard, J. F. Ferrell, L. G. Leslie, and J.-S. Lai, "Design considerations for a 48 V fuel cell to split single phase inverter system with ultracapacitor energy storage," in Proc. IEEE PESC, Jun. 23–27, 2002, vol. 2, pp. 2007–2012.
- [11] R. Gopinath, S. Kim, J.-H. Hahn, P. N. Enjeti, M. B. Yeary, and J. W.Howze, "Development of a low cost fuel cell inverter system with DSP control," IEEE Trans. Power Electron., vol. 19, no. 5, pp. 1256–1262, Sep. 2004.
- [12] J. Mazumdar, I. Batarseh, N. Kutkut, and O. Demirci, "High frequency low cost DC–AC inverter design with fuel cell source for home applications," in Proc. IEEE PES, 2002, pp. 789–794.
- [13] J. Wang, F. Z. Peng, J. Anderson, A. Joseph, and R. Buffenbarger, "Low cost fuel cell inverter system for residential power generation," in Proc. IEEE PESC, 2004, pp. 367–373.
- [14] X. Kong, L. T. Choi, and M. K. Ashwin, "Analysis & control of isolated current fed full bridge converter in fuel cell system," in Proc. 30th Annu. Conf. IEEE Ind. Electron. Soc., Busan, Korea, Nov. 2–6, 2004, pp. 2825–2830. K. Rajashekara, "Hybrid fuel-cell strategies for clean power generation,"IEEE Trans. Ind. Appl., vol. 41, no. 3, pp. 682–689, May/Jun. 2005.
- [15] M. Tanrioven and M. S. Alam, "Modeling, control, and power quality evaluation of a PEM fuel cell-based power supply system for residential use," IEEE Trans. Ind. Appl., vol. 42, no. 6, pp. 1582–1589, Nov./Dec. 2006.
- [16] A. Kirubakaran, S. Jain, and R. K. Nema, "A review on fuel cell technologies and power electronic interface," Int. J. Renew. Sustain. Energy Rev.,vol. 13, no. 9, pp. 2430–2440, Dec. 2009.
- [17] N. Mohan, T. M. Undeland, and W. P. Robbins, Power Electronics Converters, Applications and Design. Hoboken, NJ: Wiley, 2001
- [18] N. Mohan, T. M. Undeland, and W. P. Robbins, Power Electronics Converters, Applications and Design. Hoboken, NJ: Wiley, 2001
- [19] A. Kirubakaran, S. Jain, and R. K. Nema, "Dynamic modeling and simulation of PEM fuel cell," in Proc. Int. Conf. Energy Eng., Puduchery, India, Jan. 9–13, 2009, pp. 1–6.
- [20] "Fuzzy logic examples using MATLAB,"Ballal fuzzy logic notes.
- [21] "PID Controller Tuning" Jinghua Zhong